

# UCLA

## UCLA Previously Published Works

### Title

Selinexor (KPT-330) has antitumor activity against anaplastic thyroid carcinoma in vitro and in vivo and enhances sensitivity to doxorubicin.

### Permalink

<https://escholarship.org/uc/item/52f072bm>

### Journal

Scientific reports, 7(1)

### ISSN

2045-2322

### Authors

Garg, Manoj  
Kanojia, Deepika  
Mayakonda, Anand  
et al.

### Publication Date

2017-08-01

### DOI

10.1038/s41598-017-10325-x

Peer reviewed

# SCIENTIFIC REPORTS

OPEN

## Selinexor (KPT-330) has antitumor activity against anaplastic thyroid carcinoma *in vitro* and *in vivo* and enhances sensitivity to doxorubicin

Manoj Garg<sup>1,2</sup>, Deepika Kanojia<sup>1</sup>, Anand Mayakonda<sup>1</sup>, Trivadi S Ganesan<sup>2</sup>, Bindhya Sadhanandhan<sup>2</sup>, Sidhanth Suresh<sup>2</sup>, Sneha S.<sup>2</sup>, Rohit P. Nagare<sup>2</sup>, Jonathan W. Said<sup>3</sup>, Ngan B. Doan<sup>3</sup>, Ling-Wen Ding<sup>1</sup>, Erkan Baloglu<sup>4</sup>, Sharon Shacham<sup>4</sup>, Michael Kauffman<sup>4</sup> & H. Phillip Koeffler<sup>1,5</sup>

Anaplastic thyroid carcinoma (ATC) is one of the most lethal malignancies having no effective treatment. Exportin-1 (XPO1) is the key mediator of nuclear export of many tumor suppressor proteins and is overexpressed in human cancers. In this study, we examined the therapeutic potential of selinexor (XPO1 inhibitor) against human ATC cells both *in vitro* and *in vivo*. Here, we showed that XPO1 is robustly expressed in primary ATC samples and human ATC cell lines. Silencing of XPO1 by either shRNA or selinexor significantly reduced cellular growth and induced cell cycle arrest, apoptosis of ATC cells by altering the protein expression of cancer-related genes. Moreover, selinexor significantly inhibited tumor growth of ATC xenografts. Microarray analysis showed enrichment of DNA replication, cell cycle, cell cycle checkpoint and TNF pathways in selinexor treated ATC cells. Importantly, selinexor decreased AXL and GAS6 levels in CAL62 and HTH83 cells and suppressed the phosphorylation of downstream targets of AXL signaling such as AKT and P70S6K. Finally, a combination of selinexor with doxorubicin demonstrated a synergistic decrease in the cellular proliferation of several ATC cells. These results provide a rationale for investigating the efficacy of combining selinexor and doxorubicin therapy to improve the outcome of ATC patients.

Thyroid cancer is the most common endocrine malignancy and it is increasing worldwide (approximately 5 to 6% increase every year)<sup>1,2</sup>. The majority of patients with thyroid cancer has well-differentiated tumors and usually is cured by surgical resection. Anaplastic thyroid carcinomas (ATCs) are rare, accounting for less than 2% of all the thyroid malignancies. ATC is extremely aggressive with a very low cure rate, and the average 5-year survival is less than 10% with a median survival of 3 to 5 months<sup>3,4</sup>. Multimodal treatments including surgery, radiotherapy and conventional chemotherapeutic agents such doxorubicin have all been used but the clinical outcome remains dismal<sup>5</sup>. Currently, no effective treatment options are available in the clinics for patients with ATC. Therefore, development of small molecule targeted therapy will be an exciting strategy for treatment of ATC.

Exportin-1/chromosome region maintenance 1 (XPO1/CRM1) is the best-characterized nuclear export receptor, involved in the transport of more than 220 proteins as well as selected RNAs from the nucleus to the cytoplasm. XPO1 recognizes the leucine-rich nuclear export signal (NES) on proteins<sup>6–8</sup> and is an exclusive nuclear exporter of several tumor suppressors and growth regulatory proteins such as p21, p53, p73, CDKN1A, RB, BRCA1, FOXO, APC, NPM1 and STAT3<sup>9–13</sup>. Overexpression of XPO1 in cancers can lead to an imbalance of these proteins in the cytosolic compartment resulting in either inactivation of the tumor suppressor or an excess of anti-apoptotic activity (oncoprotein). Overexpression of XPO1 has been reported in leukemia<sup>14</sup>, lung cancer<sup>15</sup>,

<sup>1</sup>Cancer Science Institute (CSI) of Singapore, National University of Singapore, Singapore, Singapore. <sup>2</sup>Department of Medical Oncology and Clinical Research, Cancer Institute (WIA), Adyar, Chennai, India. <sup>3</sup>Department of Pathology and Laboratory Medicine, David Geffen School of Medicine, Los Angeles, CA, USA. <sup>4</sup>Karyopharm Therapeutics Inc, Newton, MA, 02459, USA. <sup>5</sup>Division of Hematology/Oncology, Cedars-Sinai Medical Center, University of California Los Angeles, School of Medicine, Los Angeles, CA, USA. Correspondence and requests for materials should be addressed to M.G. (email: [manoj.garg@cancerinstitutewia.org](mailto:manoj.garg@cancerinstitutewia.org) or [nuscsimg@gmail.com](mailto:nuscsimg@gmail.com))

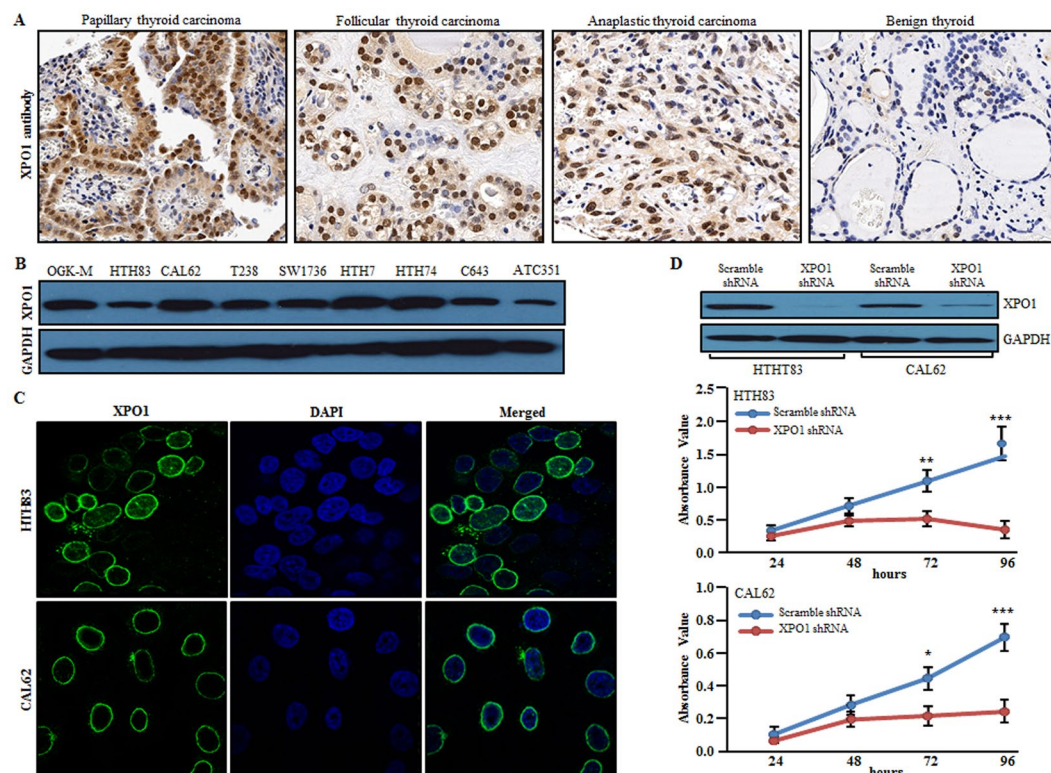


**Figure 1.** Endogenous expression of XPO1 in human ATC samples and cell lines, and effect of silencing of XPO1 in ATC cells. **(A)** Immunohistochemical analysis for detection of endogenous expression of XPO1 protein in thyroid tumors and benign thyroid tissues. Representative photographs showing nuclear staining (brown color) of XPO1 in different histological subtypes of thyroid carcinoma: papillary, follicular, ATC and benign thyroid (low or no reactivity) (original magnification,  $\times 200$ ; objective  $\times 20$ ). **(B)** Western blot analysis of ATC cell lines verified that the XPO1 antibody specifically recognizes a band of 123 kDa, corresponding to the size of XPO1 protein. **(C)** Indirect immunofluorescence assay showing nuclear localization of XPO1 protein in fixed/permeabilized ATC cell lines; DAPI stains nuclei. **(D)** ATC cells were transfected with either XPO1 shRNA or scrambled shRNA. XPO1 knockdown was confirmed in HTH83 and CAL62 cells by western blotting. GAPDH antibody was used to assure equal loading of lysates. Original and full-length blots are included in the Supplementary Information. XPO1 silencing resulted in decreased cell proliferation of HTH83 and CAL62 as measured using MTT assay. Results represent mean  $\pm$  SD;  $n = 4$ .  $*P \leq 0.01$ ;  $**p \leq 0.001$ ;  $***p \leq 0.0001$  (Student's *t*-test).

esophageal squamous cell carcinoma<sup>16</sup>, sarcoma<sup>17, 18</sup>, hepatocellular carcinoma<sup>19</sup>, melanoma<sup>20</sup> as well as multiple myeloma<sup>21</sup>. High expression of XPO1 has been positively associated with a poor prognosis and short survival in selected malignancies<sup>14, 22–25</sup>. A preliminary analysis of *in silico* data suggests that ATC has high XPO1 levels. Therefore, we hypothesized that the blockade of XPO1 by using XPO1 inhibitors may have potent activity against this cancer. Leptomycin B (LMB) is the first natural XPO1 inhibitor which possesses strong anticancer properties<sup>26, 27</sup> but its toxicity prevented it from being clinically useful<sup>28</sup>. In contrast, selinexor (KPT-330; Karyopharm Therapeutics, Newton, MA, USA) is a first-in-class, oral selective inhibitor of XPO1 resulting in blockade of nuclear export. This compound selectively binds to the Cys528 of XPO1, thereby inhibiting XPO1 binding to the NES domains of its cargo protein. Phase I trials have indicated that selinexor is well tolerated and has a favorable outcome in patients with acute myeloid leukemia<sup>29, 30</sup>. To our knowledge, no clinical trials have determined the effectiveness of selinexor against ATC. Therefore, we have examined the role of this drug in ATC to determine whether it possesses significant antitumor activity against ATC and provide rationale for conducting clinical trials of selinexor in patients with ATC. In the present study, we observed that the drug inhibited cell proliferation including clonogenic growth and induced apoptosis of ATC cells *in vitro* as well as growth of ATC xenografts. Moreover, selinexor, when combined with doxorubicin showed increased anticancer activity.

## Results

**XPO1 expression in human ATC patient samples and cell lines and effect of silencing of XPO1 in ATC cells.** We evaluated the expression of endogenous XPO1 protein in thyroid patient samples using immunohistochemistry on 39 papillary, 8 follicular, 10 anaplastic and 10 benign thyroid tissue sections using XPO1 antibodies. Nuclear staining of XPO1 was observed in 77% (30 of 39) of papillary, 75% (6 of 8) of follicular and 90% (10 of 10) of anaplastic thyroid carcinoma. In contrast, either very weak or no positive immunoreactivity of XPO1 was observed in benign thyroid tissues (Fig. 1A). Further, protein expression of XPO1 was examined in a panel of ATC cell lines (OGK-M, HTH83, CAL62, T238, SW1736, HTH7, HTH74, C643 and ATC351); and

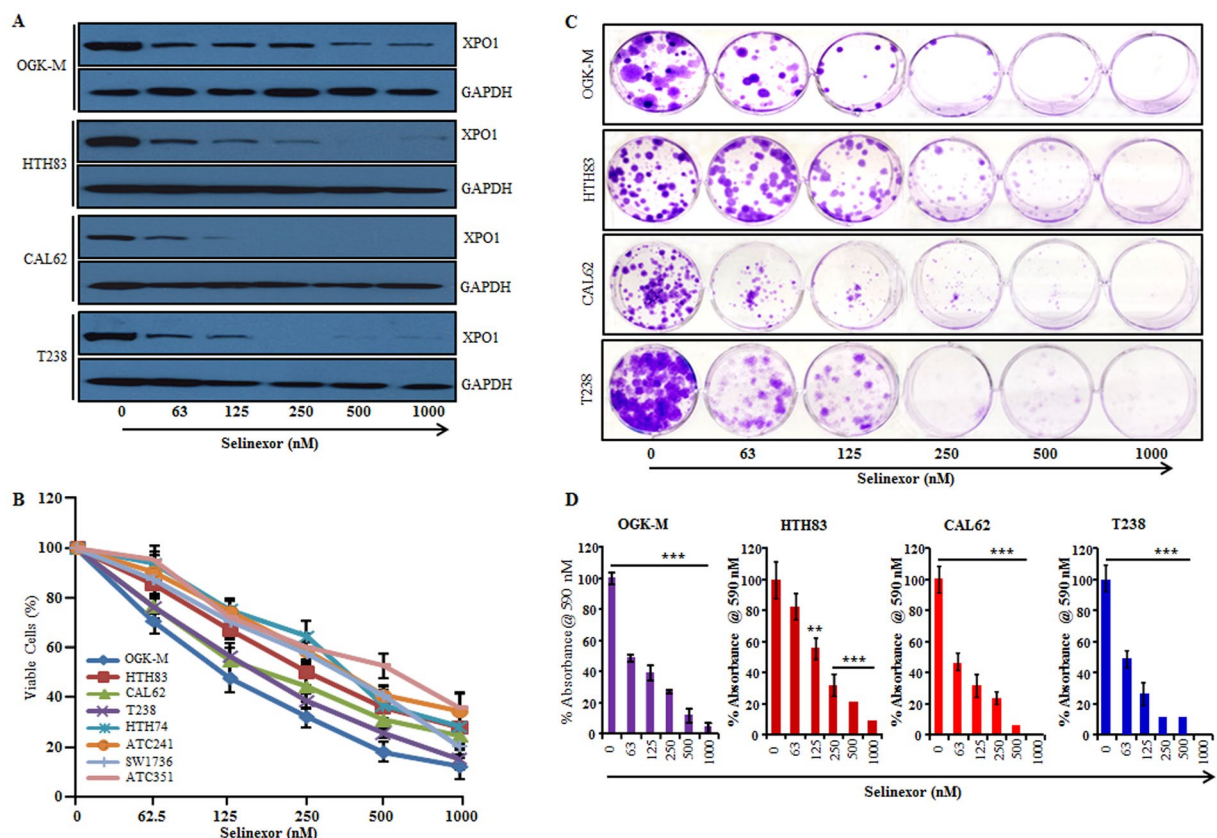


**Figure 2.** Selinexor significantly suppressed cellular growth and clonogenic ability of human ATC cells *in vitro*. (A) OGK-M, HTH83, CAL62 and T238 cells were cultured with increasing concentrations of selinexor (0–1,000 nM) for 24 h. Whole-cell lysates were prepared, and XPO1 protein expression was analyzed using western blot analysis. GAPDH was used as an internal control. Cell viability of eight human ATC cell lines. Original and full-length blots are included in the Supplementary Information. (B) Cells were treated with selinexor at indicated concentrations for 72 h, and growth inhibition was measured by MTT assay. Results are expressed as mean value  $\pm$  SD;  $n = 4$ . (C and D) Representative photomicrograph displayed that selinexor treatment decreased clonogenic growth. ATC cells were exposed to indicated concentrations of selinexor for 48 h; cells were washed with drug-free medium and allowed to form colonies for 2 weeks followed by crystal violet staining and quantification. Data represent mean  $\pm$  SD of four independent experiments done in triplicates. \* $p \leq 0.01$ ; \*\* $p \leq 0.001$ ; \*\*\* $p \leq 0.0001$  (Student's *t*-test).

each had strong XPO1 protein expression (Fig. 1B). Indirect immunofluorescence analysis showed strong nuclear localization of XPO1 protein in fixed and permeabilized ATC cells (HTH83, CAL62, T238 and OGK-M) (Fig. 1C, Supplementary Figure 1A). To determine the potential role of XPO1 in ATC, endogenous levels of XPO1 were silenced in HTH83, CAL62, OGK-M and T238 cells using shRNA targeting to XPO1. XPO1 shRNA showed 70–90% inhibition of XPO1 in these ATC cell lines both at the mRNA (Supplementary Figure 1B) and protein levels (Fig. 1D, Supplementary Figure 1C). Silencing of XPO1 resulted in a significant decrease in cell growth of ATC cells in liquid culture compared to scramble shRNA (Fig. 1D, Supplementary Figure 1D).

**Selinexor significantly suppressed cellular proliferation and clonogenic growth of human ATC cells.** Next, we examined whether selinexor could inhibit XPO1 protein expression in ATC cells *in vitro*. OGK-M, HTH83, CAL62 and T238 cells were cultured with increasing doses of selinexor (0–1000 nM) for 24 h. The small molecule inhibitor in a dose-dependent manner inhibited XPO1 protein levels in all four cell lines (Fig. 2A), but the drug had no significant effect on XPO1 mRNA levels (Supplementary Figure 2A). Selinexor in a dose-dependent manner potently inhibited the growth of a panel of ATC cell lines with IC<sub>50</sub> values between 150–500 nM in liquid culture (Fig. 2B). In contrast, the drug had no significant anti-proliferative effect against normal rat thyroid cells (FRTL5; Fischer rat thyroid cells) (Supplementary Figure 2B). Furthermore, selinexor significantly decreased the clonogenic growth of OGK-M, HTH83, CAL-62 and T238 in a dose-dependent manner (Fig. 2C and D).

**XPO1 inhibition induced cell cycle arrest and apoptosis of ATC cell lines *in vitro*.** To determine whether inhibition of cell growth was due to an alteration in the cell cycle, we analyzed cell cycle distribution of ATC cells either exposed to various concentrations (0–1000 nM, 48 h) of selinexor or XPO1 was silenced by transfection with XPO1 shRNA. XPO1 inhibition significantly increased G1 phase and decreased the S and G2/M



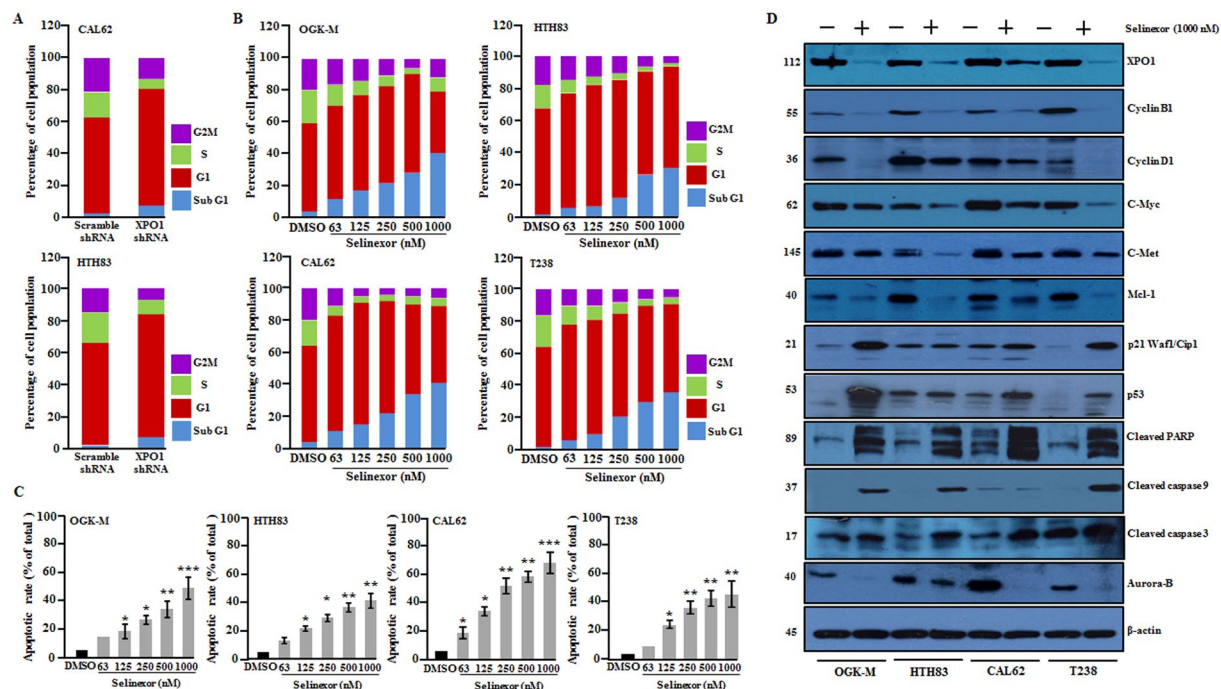


**Figure 3.** Inhibition of XPO1 induced cell cycle arrest and apoptosis of ATC cells in a dose-dependent manner. (A) Silencing of XPO1 in ATC cells resulted in an increased in G1 phase. (B) OGK-M, HTH83, CAL62, and T238 cells were treatment with either different concentrations of selinexor (0–1,000 nM) or diluent control (DMSO), stained with propidium iodide (PI) and analyzed by flow cytometric analysis. Histogram showed the proportion of cells in different phases of cell cycle. Data are presented as the mean of three independent experiments. (C) ATC cells were treated with selinexor at indicated concentrations for 24 h, stained with annexin V-FITC and PI, and subjected to flow cytometric analysis to evaluate the ability of selinexor to induce apoptosis. Histograms represent the percentage of apoptotic cells. Data are presented as mean  $\pm$  SD of three independent experiments. \* $p \leq 0.01$ ; \*\* $p \leq 0.001$ ; \*\*\* $p \leq 0.0001$  for selinexor vs. controls. (D) OGK-M, HTH83, CAL62 and T238 cells were treated with either selinexor (1,000 nM) or DMSO for 24 h. Lysates were analyzed by western blot analysis for the indicated cell cycle and apoptosis proteins (GAPDH, internal loading control). Original and full-length blots are included in the Supplementary Information.

phases in ATC cells (Fig. 3A). Of note, selinexor treatment resulted in cell cycle arrest in a dose-dependent manner (Fig. 3B, Supplementary Figure 3A). Flow cytometric analysis of OGK-M, HTH83, CAL62 and T238 cells after propidium iodide and annexin V staining showed a marked dose-dependent increase in the percentage of apoptotic cells ( $PI^{high}/AV^{high}$ ) after culture with selinexor (0–1000 nM, 48 h) (Fig. 3C, Supplementary Figure 3B). Further, we observed that selinexor altered the expression of its known cargo proteins (e.g., p53, p27 and p21), as well as indirect targets including cyclin B1, cyclin D1 in the ATC cell lines (Fig. 3D). Selinexor treatment (1000 nM, 24 h) also increased cleaved PARP, cleaved caspase-9 and cleaved caspase-3 in ATC cells (Fig. 3D). Cleavage of PARP [poly (ADP-ribose) polymerase is one of the hallmarks of apoptosis and caspase activation. This was associated with a decrease in the protein levels of anti-apoptotic proteins such as MCL1 and C-Myc (Fig. 3D). Moreover, we evaluated the dose-dependent effect of selinexor on the protein expression of a few important genes in CAL62 cells (Supplementary Figure 3C).

**Selinexor inhibits ATC growth *in vivo*.** The anti-proliferative potential of selinexor was tested *in vivo* against CAL62 human ATC xenografts growing in NSG mice (described in more detail in Material and Method Section). When xenograft tumors approached approximately 100 mm<sup>3</sup> in volume, mice started to receive either selinexor (10 mg/kg dissolved in 100  $\mu$ l of vehicle administered orally) or 100  $\mu$ l vehicle alone (3 times per week for 4 weeks). Selinexor significantly reduced mean tumor volumes and weights compared to xenograft tumors in control mice receiving vehicle (Fig. 4A and B). Western blot analysis of tumor lysates showed that proteins levels of cyclin B1 and C-Myc were reduced in tumors obtained from selinexor-treated mice as compared to those from vehicle control mice (Fig. 4C). Immunostaining of these dissected tumors displayed the significantly lower number of XPO1, Ki-67 (cell proliferation marker), and CD31 (blood vessels) positive cells in selinexor-treated mice compared to vehicle-treated mice (Fig. 4D and E). Moreover, we observed an increase in the Tunel-positive cells (increased apoptosis) in selinexor treated group (Fig. 4D and E). Importantly, selinexor-treated mice maintained normal activity, did not lose weight and had comparable levels of total white blood cells, neutrophils, haematocrit, platelet counts, serum levels of albumin, aspartate aminotransferase, alanine transaminase and creatinine compared to the vehicle group (Supplementary Table 2). Taken together, our findings provide a rationale for a therapeutic trial of selinexor for the treatment of ATC patients.

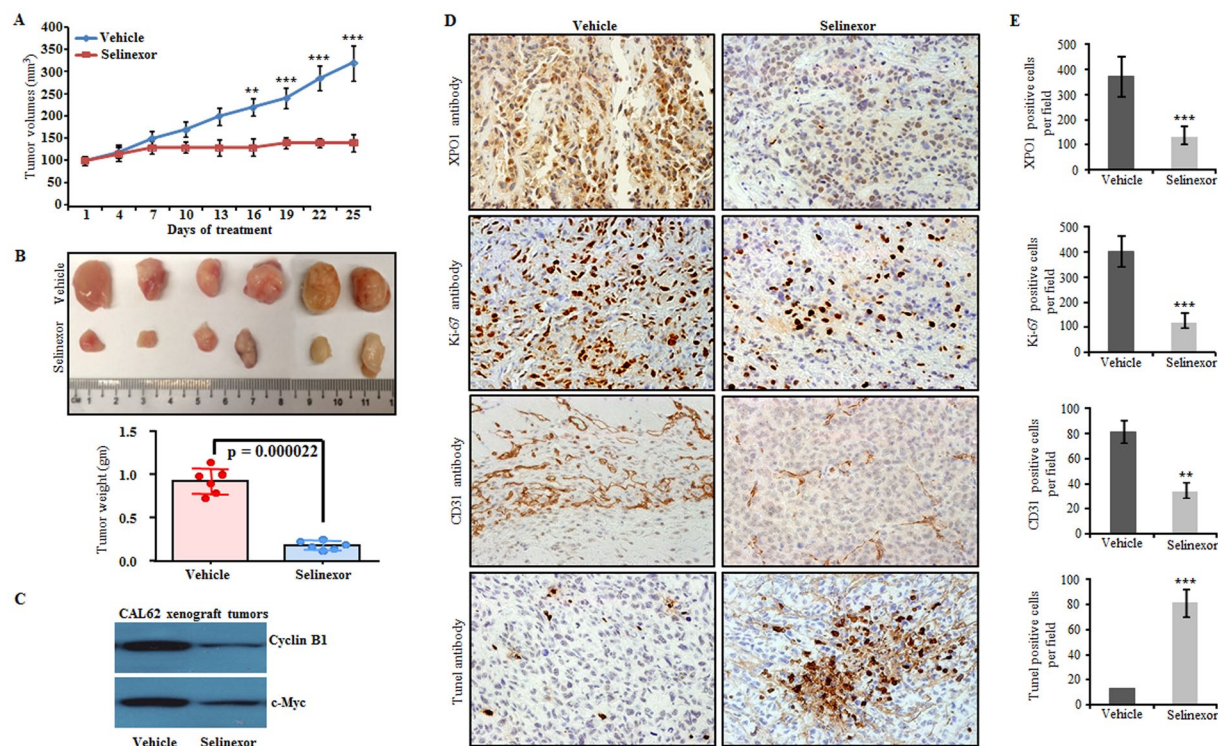


**Figure 4.** Selinexor inhibits ATC growth *in vivo*. (A) Immunodeficient mice received ATC cells (CAL62) subcutaneously. One week after implantation, mice began to receive either oral selinexor (10 mg/kg, 3 times per week for 4 weeks) or vehicle alone. Selinexor treatment significantly suppressed tumor volumes (mean  $\pm$  SD of 6 tumors).  $*P \leq 0.01$ ;  $**P \leq 0.001$ ;  $***P \leq 0.0001$  (Student's t-test). (B) Representative photograph showing decreased tumor growth in selinexor treated group compared to vehicle treated group ( $n = 6$  for each group). Scale in cm. (Lower panel) Tumor weights from selinexor and vehicle treated groups (mean  $\pm$  SD of 6 tumors,  $P = 0.000022$ ). (C) At the end of the experiment, whole cell lysates (protein) were prepared from tumors resected from selinexor-treated and vehicle-treated mice and subjected to western blotting with indicated antibodies. (D and E) Tumor sections were subjected to immunohistochemical analysis. Tumors section from the selinexor-treated group showed weak staining for XPO1 (exportin 1), cell proliferation marker (Ki-67) and blood vessel marker (CD31) and strong staining for Tumor (a marker of apoptosis) as compared to vehicle-treated group original magnification,  $\times 200$ ; objective  $\times 20$ ). Columns (on the right) represent mean  $\pm$  SD of three independent tumors.  $**P \leq 0.001$ ;  $***P \leq 0.0001$  (Student's t-test).

**Effect of selinexor on gene expression profiling of ATC cells.** To study global transcriptome changes resulting from inhibition of XPO1, gene expression profiling of OGC-M and HTH83 cells after 12 hours exposure to selinexor or DMSO was performed using microarray. Gene expression analysis found that 2491 (FDR  $< 0.05$ ) genes were differentially expressed upon selinexor treatment across 2 cell lines compared to their DMSO group (Fig. 5A). Gene set enrichment analysis (GSEA) showed significant negative enrichment in the cell cycle, Aurora kinase pathways and positive enrichment of tumor necrosis factor (TNF) pathway (Fig. 5B–E). Further, we analyzed expression of cell cycle genes using publicly available microarray database GSE9115. We found that ATC tumor samples had higher expression of cell cycle genes than normal thyroid samples<sup>31</sup> (Supplementary Figure 4). Reliability of the microarray data was further verified using quantitative RT-PCR for 12 randomly selected genes. Expression levels of *CCNB1*, *CCNB2*, *AURKA*, *AURKB*, *AXL*, *MET* were significantly downregulated, whereas mRNA levels of *TNF*, *IL-6*, *CASP3*, *SMAD7*, *KLF6* were significantly upregulated in selinexor treated HTH83 cells compared to vehicle (Fig. 5F). These results were consistent with the microarray data. Taken together, these results showed that selinexor have a moderate effect on cell cycle and DNA replication of ATC cells.

**Selinexor suppresses AXL signaling in ATC cells.** TYRO3 and AXL receptor tyrosine kinases and their ligand GAS6 are expressed in several types of the tumor including ATC, and AXL signaling has a key role in cell proliferation, migration, invasion, adhesion and survival<sup>32–34</sup>. Our microarray data showed that AXL and GAS6 were down-regulated in selinexor treated cells and was confirmed at the mRNA level in ATC cells (Fig. 5F). We, therefore, chose to examine whether selinexor inhibits protein levels of AXL in ATC cells. Interestingly, we found that selinexor treatment not only suppressed AXL protein levels but also resulted in attenuation of the PI3K pathway (phosphorylation of AKT and p70S6 kinase) in ATC cell lines (Fig. 6A).

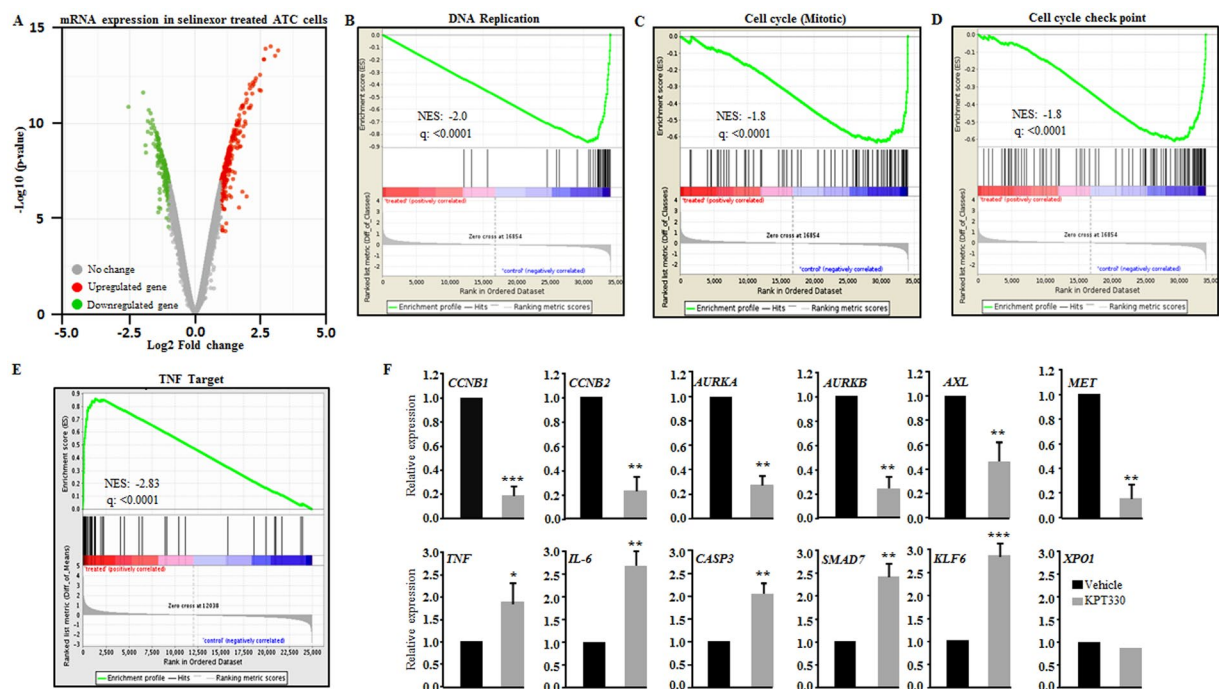


**Figure 5.** Effect of selinexor on gene expression profiling of ATC cells. (A) Volcano plot shows differentially expressed genes for OGK-M cells treated with either vehicle (DMSO) or 1,000 nM selinexor for 12 h. Red and green dots represent up-regulated and down-regulated genes, respectively. Grey dots represented no change. (B–E) Gene set enrichment analysis showed negative enrichment of DNA replication, cell cycle, cell cycle checkpoint and positive enrichment of TNF (tumor necrotic factor) target pathway. (F) qRT-PCR validation of 12 selected genes identified as differentially expressed by microarray. Expression of each gene was normalized to *GAPDH* as a reference (control value converted to 1). Figures are representative of 3 replicates. Data represent mean  $\pm$  SD,  $n = 3$ . \*\* $p \leq 0.001$ , \*\*\* $p \leq 0.0001$ . NES indicates normalized enrichment score; and  $q$  = false discovery rate.

**Selinexor effectively enhances growth arrest of ATC cells in combination with doxorubicin.** Next, we examined whether selinexor could enhance the effect of the chemotherapeutic agents currently used to treat ATC. Doxorubicin and paclitaxel are FDA approved drugs for the treatment of ATC patients in the clinic<sup>5</sup> and therefore a combination of these drugs with selinexor are of particular interest in ATC. In agreement with the prior study, we found doxorubicin had a similar inhibitory effect on HTH83, CAL62 SW176, ATC351 cell lines, with an IC<sub>50</sub> about 100 to 200 nM (Fig. 6B and C, Supplementary Figure 5B and E). Notably, we observed that combination of selinexor and doxorubicin produced synergistic growth inhibitory activity against HTH83, CAL62, SW1736 and ATC351 cells (Fig. 6B–F Supplementary Figure 5A–F). The combination effect is more effective in SW1736 and ATC351 cells compared to HTH83 and SW1736 cells. Overall, our results indicate that combination of selinexor and doxorubicin might be a potential therapeutic option for targeting ATC. This combination warrants further preclinical and clinical development against ATC.

## Discussion

ATC is a devastating malignancy which is extremely aggressive and resistant to available chemotherapy<sup>2,5,35,36</sup>. Targeted therapies against proteins which are altered in ATC may hold the key to designing effective treatment for this fatal malignancy. The nucleo-cytoplasmic transport of proteins is crucial for maintaining normal cellular functions. The process relies on the exportins. XPO1 transports a large number proteins and RNAs across the nuclear envelope<sup>37</sup>. Increased expression of XPO1 occurs with the progression of several types of cancers and therefore is an attractive protein for targeted molecular therapy in ATC.

To the best of our knowledge, the present study is the first to verify overexpression of XPO1 protein in human ATC samples and cell lines compared to benign thyroid diseases. Immunofluorescence data also support that XPO1 is robustly expressed in the nucleus of the ATC cell lines. Further, knockdown of XPO1 suppressed the cellular proliferation of several ATC cell lines in liquid culture. Taken together, these data suggest that overexpression of XPO1 may have a potential role in the pathogenesis of ATC. Recently, several studies showed that Selective Inhibitor of Nuclear Export (SINE) compounds have anti-tumor activities with acceptable toxicities<sup>15,17–19,38</sup>. Selinexor is an orally available advanced selective inhibitor of XPO1 and is currently being investigated in phase I/II clinical trials in patients with advanced solid tumors and hematologic malignancies<sup>30,39</sup>. Selinexor treatment leads to growth inhibition in liquid culture and markedly suppressed clonogenic ability, as well as decreased tumor growth in ATC xenograft model<sup>15,19,20</sup>. Flow cytometric analysis demonstrated that selinexor treatment induced cell-cycle arrest and apoptosis in several ATC cells *in vitro*. Selinexor treatment markedly altered protein



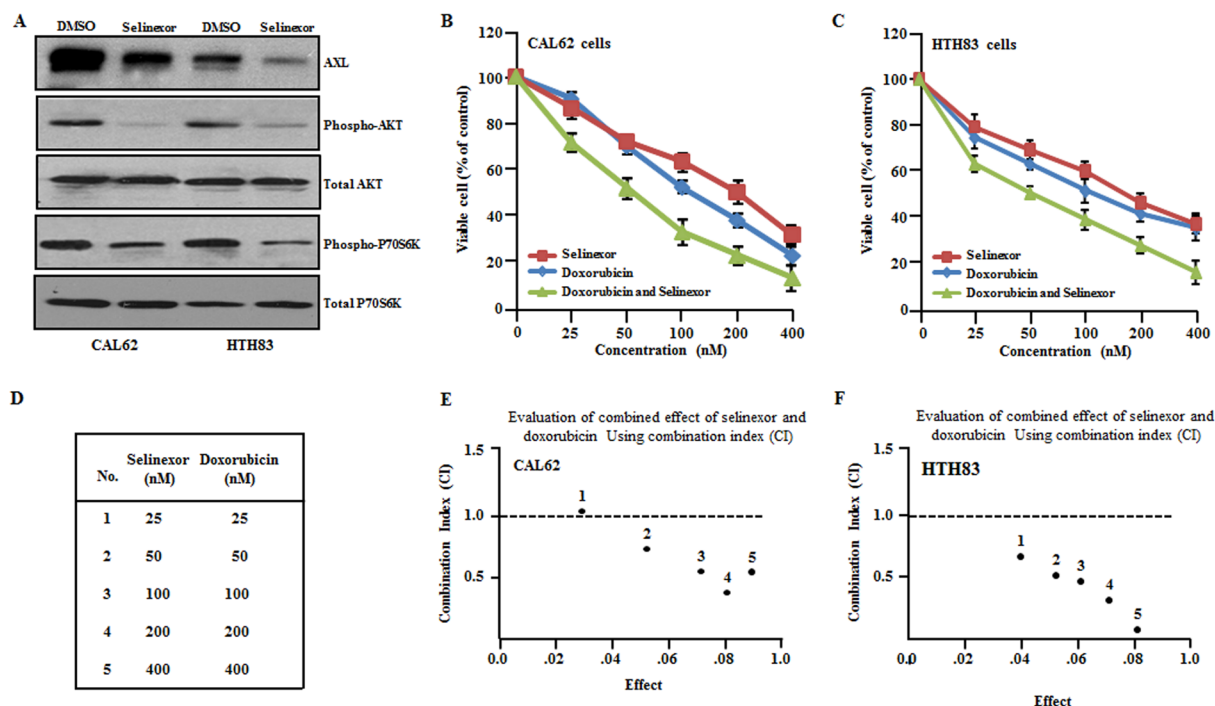


**Figure 6.** Selinexor suppressed AXL signaling, and the drug effectively enhanced growth arrest of ATC cells in combination with doxorubicin. (A) HTH83 and CAL62 cells were cultured with either selinexor (1,000 nM) or diluent control (DMSO) for 24 h, and the whole-cell lysate was subjected to western blot analysis for AXL, p-AKT, total AKT, p-P70S6K and total P70S6K. (B and C) Proliferation study of the combination of selinexor with doxorubicin. Data represent means  $\pm$  s.d.;  $n = 3$ . (D–F) Combinational growth inhibition of selinexor and doxorubicin on CAL62 and HTH83 cells displayed as CI. CI defines the interaction between selinexor and doxorubicin as plotted against a fraction of cell viability.  $CI < 1$ ,  $CI = 1$  and  $CI > 1$  represent synergism, additive, and antagonism of the two compounds, respectively.

expression related to cell cycle arrest through upregulation of p53 and p27, and downregulation of cyclin B1, cyclin D1 as well as apoptosis-related proteins including upregulation of cleaved caspase 3, cleaved PARP and cleaved caspase 9 as well as annexin V positive staining in ATC cells *in vitro*. Most importantly, selinexor treatment (10 mg/kg, three times per week) leads to inhibition of tumor growth in ATC xenografts, which was associated with their decreased proliferation (Ki-67), blood vessel formation (CD31) and increased apoptosis (Tunel staining). These observations were consistent with our *in vitro* findings and also similar to previously published reports concerning the effect of selinexor on other malignancies<sup>15, 19, 40, 41</sup>.

Our microarray analysis also showed that selinexor significantly enriched for pathways related to DNA replication, cell cycle, cell cycle checkpoint and TNF upon treatment of OGK-M ATC cells with selinexor. Taken together, the data suggested that selinexor has a profound effect on the expression of genes involved in cellular growth, DNA replication, cell cycle and apoptosis of ATC cells. The transcription factor C-Myc and the tyrosine kinase receptor C-Met were highly expressed in ATC and play a vital role in their progression<sup>42, 43</sup>. Even though neither C-Myc nor C-Met are direct XPO1 target proteins, but selinexor indirectly reduced levels of C-Myc and C-met proteins. Of note, previous studies of multiple myeloma and hepatocellular carcinoma also observed a reduction in the C-Myc and C-Met levels following Selective Inhibitor of Nuclear Export (SINE) treatment of these cells<sup>19, 21, 44</sup>.

Previous studies showed that AXL/TYRO3 and GAS6 play a critical role in ATC progression and survival<sup>32</sup>. Our microarray, qRT-PCR and western blot data verified that selinexor treatment suppressed AXL expression in ATC cells. Moreover, we observed that selinexor treatment leads to decreased phosphorylation of downstream targets of AXL signaling such as AKT and P70S6K. How selinexor suppresses AXL signaling requires further investigation. Moreover, our results demonstrated that the combination of selinexor with doxorubicin synergistically enhanced the anti-proliferative activity of selinexor. This observation is consistent with earlier studies in other human malignancies<sup>45</sup>. Recently, phase I/II clinical trials of selinexor in combination with doxorubicin are ongoing for several malignancies.

In summary, our studies showed for the first time that selinexor either alone or in combination with doxorubicin may be effective in the treatment of ATC patients. These studies identify the opportunities for future clinical trials for ATC patients.

## Materials and Methods

**Cell culture.** Human ATC cell lines: T238 and CAL62 were kind gifts from L. Roque (Instituto Português de Oncologia, Lisboa, Portugal) and Dr. J. Giovanni (Centre Antoine-Lacassagne, Nice, France), respectively. OGK-M



	Thyroid Carcinoma cell lines								
	HTH83*	CAL62**	SW1736**	OGK-M***	ATC351**	C643**	HTH7**	HTH74**	T238**
vWA	16,19	16	16,19	17	18	15,17	14,18	16,17	16,17
TPOX	8	8,9	11	8,9	8,11	11,12	11	8,10	8,11
TH01	6,9	7,9	6,9,3	6,10	7	9,3,10	9,9,3	8	7,9,3
D5S818	12	9,12	12,13	10,13	12,13	11,12	11	11,12	9,11
D13S317	11,13	12	11,12	10,12	11	8,10	11,14	12,13	12
D7S820	12	10	8,11	10,13	9,10	9,12	8,11	9	11,13
D16S539	11,12	12,13	11,12	9,12	9,11	9,13	9,13	9	11,12
CSF1PO	11	9,12	12	10,11	12	10,11	12	11,12	12, 13
AMEL	XY	X	X	XY	XY	XY	X	X	X

**Table 1.** STR profiling of thyroid carcinoma cell lines. \*STR profile by us matched to ATCC results. \*\*STR profile by us matched to University of Kentucky (Lexington), University of Uppsala (Sweden), University of Colorado Cancer Centre and Memorial Sloan-Kettering Cancer Centre. \*\*\*STR profile matched to original profile (33).

cells were established in H. Phillip Koeffler laboratory<sup>46</sup>. HTH83, SW1736, C643, HTH7 and HTH74 were generously obtained from Dr. K. Ain (University of Kentucky, Lexington, KY) with permission from Dr. Nils-Erik Heldin (University of Uppsala, Sweden). All cell lines were cultured and maintained in RPMI1640 containing 10% fetal bovine serum (FBS) and 1% penicillin-streptomycin (Invitrogen, Carlsbad, CA) at 37 °C in a humidified atmosphere with 5% CO<sub>2</sub>. FRTL5 cells (Fischer rat thyroid cells) were maintained in Ham's F12K medium, 5% FBS, 1% penicillin-streptomycin (Invitrogen, Carlsbad, CA), 2 mM l-glutamine, 5 µg/ml insulin, 5 µg/ml transferrin, 10 nM hydrocortisone, 10 ng/ml somatostatin and 1 mU/ml thyroid stimulating hormone (TSH). STR profiling of our cell lines was done using the Genetic Resources Core Facility, UCLA, Los Angeles, CA; profiles matched to published STR profiles of ATC cell lines (Table 1)<sup>46</sup>.

**Reagent and antibodies.** Selinexor (KPT-330) and Pluronic F-68 were obtained from Karyopharm Therapeutics (Newton, MA, USA). For *in vitro* administration, selinexor was dissolved in dimethyl sulfoxide (Sigma-Aldrich) to a concentration of 20 mM/L. For *in vivo* administration, selinexor was dissolved in 0.6% w/v aqueous Pluronic F-68 (Karyopharm Therapeutics, Newton, MA, USA). Antibodies to XPO1/CRM1 (H300), C-Myc, p27 (C-19), p53 (DO-1), Bax (N20), cyclin D1 (A-12) were from Santa Cruz Biotechnologies (Dallas, TX, USA). Antibodies against p21, MCL1, cleaved PARP, cleaved caspase-9, cleaved caspase-3, Aurora-B, AXL, total AKT, p-AKT, total P70S6K, p-P70S6K and GAPDH were purchased from Cell Signaling Technology (Danvers, MA, USA). Antibody against β-actin was from Sigma-Aldrich.

**Immunohistochemistry (IHC).** IHC was performed by standard procedures as described previously<sup>46–48</sup>. Briefly, tumor tissues were fixed in formalin, embedded in paraffin and cut into 4 µm thick sections. Endogenous peroxidase activity was blocked using 3% hydrogen peroxide (H<sub>2</sub>O<sub>2</sub>), and antigen retrieval was carried out in citrate buffer. Sections were blocked using 3% normal goat serum at room temperature for 40 minutes and incubated with primary antibodies against XPO1, CD31, Ki-67 and also for Tunel assay. Immunostaining was assessed by counting >500 cells from 5 randomly selected fields of each section using a microscope (Olympus, Tokyo, Japan) at ×200 magnification as described previously<sup>46, 48</sup>.

**Western blot analysis.** Cell lysates were prepared using M-PER Mammalian protein extraction reagent (Thermo Scientific, Rockford, USA) containing 1X protease cocktail inhibitor (Roche). Western blots were performed as described previously<sup>47, 49</sup>.

**cDNA synthesis and quantitative real-time PCR (qRT-PCR).** Total RNA was isolated from ATC cell lines (CAL62, HTH83 and OGK-M) using the RNeasy mini kit (Qiagen GmbH, Hilden, Germany) according to manufacturer's protocol. 1 µg of total RNA was used for complementary DNA (cDNA) synthesis using cDNA synthesis kit (Life Technologies Inc., Gaithersburg, MA, USA). qRT-PCR was performed using KAPA SYBR master mix (Kapa-Biosystems, USA) in an ABI 7500 Fast real-time PCR system (Applied Biosystems, USA). The primers used for qRT-PCR for selected genes are shown in Supplementary Table 1.

**Indirect immunofluorescence assay.** XPO1 protein expression was confirmed in OGK-M, HTH83, CAL62 and T238 cells using immunofluorescence as described earlier<sup>16</sup>. Briefly, cells were fixed with 4% paraformaldehyde in PBS pH 7.4 for 10 minutes, washed three times with PBS and incubated with rabbit polyclonal XPO1 antibody (1:500 dilution) at room temperature for 1 h. Cells were washed and incubated with secondary antibody anti-rabbit IgG conjugated with Alexa Fluor 488 (Life Technologies, USA). 4',6-diamidino-2-phenylindole (DAPI; Sigma-Aldrich, St. Louis, MO) was used to stain the nucleus of the cells. The slides were finally washed and mounted in mounting medium (Sigma-Aldrich, St. Louis, MO), and images were captured using Nikon microscope (Nikon, Fukok, Japan).

**Short hairpin RNA (shRNA) interference.** To obtained XPO1 knockdown in HTH83, OGKM, CAL62 and T238 cells, human XPO1 shRNA (5'-GCTCAAGAAGTACTGACACAT-3') were cloned in the pLKO.1 lentiviral vector. Briefly, 293 T cells (2 × 10<sup>6</sup>) were seeded in 100 mm dish, one day before transfection in DMEM

medium supplemented with 10% FBS for virus production. To generate lentivirus particle, 2 µg of (scrambled shRNA or XPO1 shRNA) vector was transfected along with 1.5 µg of pCMV-dr8.2 and 0.5 µg of pMD2.G in 293 T cells in 100 mm culture dish using lipofectamine transfection reagent streptomycin (Invitrogen, Carlsbad, CA). After 4 hours, the transfection medium was replaced with DMEM medium supplemented with 10% FBS. Cell culture supernatants containing the lentivirus were collected at 48 h and 72 h post-transfection and pooled. HTH83, OGKM, CAL62 and T238 cells ( $1 \times 10^5$  per well) were seeded in 6-well plate 24 h before transduction. Cells were transduced with lentiviral vectors at an MOI of 30 in the presence of 8 µg/ml polybrene (Sigma-Aldrich) for 24 h. Puromycin was used to eliminate uninfected cells, stable cells were selected using 1 µg/ml puromycin for 2–3 weeks.

**Cellular proliferation assay.** Cell growth was measured by colorimetric assays as described earlier<sup>16,47</sup>. Briefly, 20 µl, 3-(4,5-dimethylthiazol-2-yl)-2,5-diphenyltetrazolium bromide (MTT; Sigma-Aldrich) was added to each well of 96 well-plate and incubated at 37 °C for 2 h and then dissolved in 100 µl of stop solution (SDS-HCl). Absorbance was measured at 570 nm using a Tecan Infinite 200 PRO spectrophotometer (Mannedorf, Switzerland). Dose-response curves were plotted to obtained half-maximal inhibitory concentrations (IC<sub>50</sub>) for selinexor by GraphPad Software.

**Colony formation assay.** ATC cells ( $1 \times 10^3$ ) were seeded into 6-well plates in triplicates in complete medium. After two days, media were supplemented with varying concentration of selinexor. After 2 weeks, cells were fixed with 5% glutaraldehyde in PBS and stained with 0.1% crystal violet. Moreover, colonies were dissolved in 200 µl of DMSO and absorbance was measured at 570 nm Tecan Infinite 200 PRO spectrophotometer. Soft agar assay (anchorage-independent growth assay) was performed as described previously<sup>47</sup>.

**Annexin V and propidium iodide (Annexin V-PI) apoptosis analysis.** Annexin V-PI staining was performed using flow cytometric analysis as previously described<sup>50</sup>. Briefly,  $1 \times 10^6$  cells were cultured with increasing concentrations of selinexor (0–1000) for 24 h. Staining was performed using Apoptosis Detection Kit II (BD Biosciences, USA). Cells were harvested and washed twice with phosphate-buffered saline (PBS; Life technologies, USA). Cells were suspended in 1X binding buffer containing 5 µl of FITCI conjugated Annexin V and 5 µl of PI for 30 min in dark. The samples were analyzed using LSR-II flow cytometer (BD, San Jose, CA, USA).

**Cell cycle analysis.** To determine the effect of selinexor on cell cycle of ATC cells, cells were seeded at 50% confluency and after overnight incubation, culture media were replaced with fresh medium either diluent control or indicated concentrations of selinexor at indicated time points as described earlier<sup>50</sup>. Briefly, cells were washed with ice-cold PBS and fixed with 70% chilled ethanol. Cells were stained with PI solution (50 µg/ml PI, Triton X-100 (1%), 20 µg/ml DNase-free RNase A in PBS) for 30 min at 37 °C in the dark followed by flow cytometric analysis (BD, San Jose, CA, USA).

**In vivo xenografts.** The response of human ATC tumors to selinexor was examined using NSG mice as previously described<sup>47</sup>. Suspensions of  $2 \times 10^6$  CAL62 cells mixed with matrigel (1:1) in 200 µl of total volume were injected subcutaneously into the right flank of 6-week male NSG mice. The mice were randomly divided into two groups (6 mice per group) to receive either vehicle (0.6% w/v aqueous Pluronic F-68) or selinexor (10 mg/kg in 100 µl of the vehicle, 3 times per week). Tumor diameters were measured with a caliper, and tumor volumes were calculated by the formula ( $V = \pi/6 \times DI \times Ds^2$ )<sup>48</sup>, where V is volume, DI is the largest diameter, and Ds is the smallest diameter. Mice were fed with Nutri-Cal (Tomlyn) thrice a week during treatment to provide good nutrition<sup>15</sup>. All mice were sacrificed at the end of the study. Tumors were dissected and weighed. One-half of each tumor was fixed in 10% formaldehyde for histological analysis, and the other half was immediately kept in –80 °C for subsequent RNA and protein analysis. We also analyzed peripheral blood for blood counts and serum chemistries after the 28-day treatment (Table 1). The animal studies were approved by the National University of Singapore (NUS) Institutional Animal Care and Use Committee (IACUC) and all the procedure were performed in accordance with the relevant guidelines and regulations.

**Microarray and data analysis.** Total RNA was isolated from three different clones in each group (groups: scrambled shRNA and LAMC2 shRNA) using the RNeasy mini kit (Qiagen, Valencia, CA) according to manufacturer's protocol. RNA Nano chip on Agilent Bioanalyzer 2100 (Agilent Technologies, Inc., Santa Clara, CA) was used to check quality and quantity of RNA samples. cDNA and cRNA were synthesized using Illumina Total Prep RNA Amplification Kit (Illumina). Human gene HT-12 v4 Expression beads a chip kit (47,000 probes spotted genes) was from Illumina (Santa Clara, CA) were used.

**Studies of drug combination.** Results obtained from MTT assays for different combinations of selinexor and doxorubicin was evaluated by CalcuSyn (Biosoft, UK). A combination index (CI) plot is a Fa-CI plot in which  $CI < 1$ ,  $= 1$ ,  $> 1$  indicate synergism, additive effect, and antagonism, respectively. Fa: the fraction that is inhibited by the drug.

**Statistics Analysis.** For *in vitro* and *in vivo* experiments, we evaluated the statistical significance of the difference between two groups using two-tailed Student t-test and two-way ANOVA. Asterisks in the figures represent significant differences between experimental groups in comparison to controls (\* $p < 0.01$ , \*\* $p < 0.001$ , \*\*\* $p < 0.0001$ ). Data points in figures represent the means  $\pm$  SD (standard deviation).

## References

- Robbins, J. *et al.* Thyroid cancer: a lethal endocrine neoplasm. *Annals of internal medicine* **115**, 133–147 (1991).
- Ain, K. B. Anaplastic thyroid carcinoma: behavior, biology, and therapeutic approaches. *Thyroid: official journal of the American Thyroid Association* **8**, 715–726 (1998).
- Sherman, S. I. Thyroid carcinoma. *Lancet* **361**, 501–511 (2003).
- O'Neill, J. P. & Shaha, A. R. Anaplastic thyroid cancer. *Oral oncology* **49**, 702–706, doi:[10.1016/j.oraloncology.2013.03.440](https://doi.org/10.1016/j.oraloncology.2013.03.440) (2013).
- Perri, F., Lorenzo, G. D., Scarpati, G. D. & Buonerba, C. Anaplastic thyroid carcinoma: A comprehensive review of current and future therapeutic options. *World journal of clinical oncology* **2**, 150–157, doi:[10.5306/wjco.v2.i3.150](https://doi.org/10.5306/wjco.v2.i3.150) (2011).
- Fornerod, M., Ohno, M., Yoshida, M. & Mattaj, I. W. CRM1 is an export receptor for leucine-rich nuclear export signals. *Cell* **90**, 1051–1060 (1997).
- Fukuda, M. *et al.* CRM1 is responsible for intracellular transport mediated by the nuclear export signal. *Nature* **390**, 308–311, doi:[10.1038/36894](https://doi.org/10.1038/36894) (1997).
- Xu, D., Grishin, N. V. & Chook, Y. M. NESdb: a database of NES-containing CRM1 cargoes. *Molecular biology of the cell* **23**, 3673–3676, doi:[10.1091/mbc.E12-01-0045](https://doi.org/10.1091/mbc.E12-01-0045) (2012).
- Freedman, D. A. & Levine, A. J. Nuclear export is required for degradation of endogenous p53 by MDM2 and human papillomavirus E6. *Molecular and cellular biology* **18**, 7288–7293 (1998).
- Sato, N. *et al.* Nuclear retention of STAT3 through the coiled-coil domain regulates its activity. *Biochemical and biophysical research communications* **336**, 617–624, doi:[10.1016/j.bbrc.2005.08.145](https://doi.org/10.1016/j.bbrc.2005.08.145) (2005).
- Rodriguez, J. A., Span, S. W., Ferreira, C. G., Krut, F. A. & Giaccone, G. CRM1-mediated nuclear export determines the cytoplasmic localization of the antiapoptotic protein Survivin. *Experimental cell research* **275**, 44–53, doi:[10.1006/excr.2002.5492](https://doi.org/10.1006/excr.2002.5492) (2002).
- Latre de Late, P. *et al.* Glucocorticoid-induced leucine zipper (GILZ) promotes the nuclear exclusion of FOXO3 in a Crm1-dependent manner. *The Journal of biological chemistry* **285**, 5594–5605, doi:[10.1074/jbc.M109.068346](https://doi.org/10.1074/jbc.M109.068346) (2010).
- Parikh, K., Cang, S., Sekhri, A. & Liu, D. Selective inhibitors of nuclear export (SINE)—a novel class of anti-cancer agents. *Journal of hematology & oncology* **7**, 78, doi:[10.1186/s13045-014-0078-0](https://doi.org/10.1186/s13045-014-0078-0) (2014).
- Kojima, K. *et al.* Prognostic impact and targeting of CRM1 in acute myeloid leukemia. *Blood* **121**, 4166–4174, doi:[10.1182/blood-2012-08-447581](https://doi.org/10.1182/blood-2012-08-447581) (2013).
- Sun, H. *et al.* KPT-330 has antitumour activity against non-small cell lung cancer. *British journal of cancer* **111**, 281–291, doi:[10.1038/bjc.2014.260](https://doi.org/10.1038/bjc.2014.260) (2014).
- Lin, D. C. *et al.* Genomic and molecular characterization of esophageal squamous cell carcinoma. *Nature genetics* **46**, 467–473, doi:[10.1038/ng.2935](https://doi.org/10.1038/ng.2935) (2014).
- Sun, H. *et al.* CRM1 Inhibition Promotes Cytotoxicity in Ewing Sarcoma Cells by Repressing EWS-FLI1-Dependent IGF-1 Signaling. *Cancer research* **76**, 2687–2697, doi:[10.1158/0008-5472.CAN-15-1572](https://doi.org/10.1158/0008-5472.CAN-15-1572) (2016).
- Garg, M. *et al.* Molecular mechanism and therapeutic implications of selinexor (KPT-330) in liposarcoma. *Oncotarget* **8**, 7521–7532, doi:[10.18632/oncotarget.13485](https://doi.org/10.18632/oncotarget.13485) (2017).
- Zheng, Y. *et al.* KPT-330 inhibitor of XPO1-mediated nuclear export has anti-proliferative activity in hepatocellular carcinoma. *Cancer chemotherapy and pharmacology* **74**, 487–495, doi:[10.1007/s00280-014-2495-8](https://doi.org/10.1007/s00280-014-2495-8) (2014).
- Pathria, G., Wagner, C. & Wagner, S. N. Inhibition of CRM1-mediated nucleocytoplasmic transport: triggering human melanoma cell apoptosis by perturbing multiple cellular pathways. *The Journal of investigative dermatology* **132**, 2780–2790, doi:[10.1038/jid.2012.233](https://doi.org/10.1038/jid.2012.233) (2012).
- Tai, Y. T. *et al.* CRM1 inhibition induces tumor cell cytotoxicity and impairs osteoclastogenesis in multiple myeloma: molecular mechanisms and therapeutic implications. *Leukemia* **28**, 155–165, doi:[10.1038/leu.2013.115](https://doi.org/10.1038/leu.2013.115) (2014).
- Yao, Y. *et al.* The expression of CRM1 is associated with prognosis in human osteosarcoma. *Oncology reports* **21**, 229–235 (2009).
- Shen, A. *et al.* Expression of CRM1 in human gliomas and its significance in p27 expression and clinical prognosis. *Neurosurgery* **65**, 153–159; discussion 159–160, doi:[10.1227/01.NEU.0000348550.47441.4B](https://doi.org/10.1227/01.NEU.0000348550.47441.4B) (2009).
- Noske, A. *et al.* Expression of the nuclear export protein chromosomal region maintenance/exportin 1/Xpo1 is a prognostic factor in human ovarian cancer. *Cancer* **112**, 1733–1743, doi:[10.1002/cncr.23354](https://doi.org/10.1002/cncr.23354) (2008).
- Gravina, G. L. *et al.* Nucleo-cytoplasmic transport as a therapeutic target of cancer. *Journal of hematology & oncology* **7**, 85, doi:[10.1186/s13045-014-0085-1](https://doi.org/10.1186/s13045-014-0085-1) (2014).
- Kudo, N. *et al.* Leptomycin B inactivates CRM1/exportin 1 by covalent modification at a cysteine residue in the central conserved region. *Proceedings of the National Academy of Sciences of the United States of America* **96**, 9112–9117 (1999).
- Mutka, S. C. *et al.* Identification of nuclear export inhibitors with potent anticancer activity *in vivo*. *Cancer research* **69**, 510–517, doi:[10.1158/0008-5472.CAN-08-0858](https://doi.org/10.1158/0008-5472.CAN-08-0858) (2009).
- Newlands, E. S., Rustin, G. J. & Brampton, M. H. Phase I trial of elactocin. *British journal of cancer* **74**, 648–649 (1996).
- Abdul Razak, A. R. *et al.* First-in-Class, First-in-Human Phase I Study of Selinexor, a Selective Inhibitor of Nuclear Export, in Patients With Advanced Solid Tumors. *Journal of clinical oncology: official journal of the American Society of Clinical Oncology* **34**, 4142–4150, doi:[10.1200/JCO.2015.65.3949](https://doi.org/10.1200/JCO.2015.65.3949) (2016).
- Gounder, M. M. *et al.* Phase IB Study of Selinexor, a First-in-Class Inhibitor of Nuclear Export, in Patients With Advanced Refractory Bone or Soft Tissue Sarcoma. *Journal of clinical oncology: official journal of the American Society of Clinical Oncology* **34**, 3166–3174, doi:[10.1200/JCO.2016.67.6346](https://doi.org/10.1200/JCO.2016.67.6346) (2016).
- Salvatore, G. *et al.* A cell proliferation and chromosomal instability signature in anaplastic thyroid carcinoma. *Cancer research* **67**, 10148–10158, doi:[10.1158/0008-5472.CAN-07-1887](https://doi.org/10.1158/0008-5472.CAN-07-1887) (2007).
- Avilla, E. *et al.* Activation of TYRO3/AXL tyrosine kinase receptors in thyroid cancer. *Cancer research* **71**, 1792–1804, doi:[10.1158/0008-5472.CAN-10-2186](https://doi.org/10.1158/0008-5472.CAN-10-2186) (2011).
- Ito, T. *et al.* Expression of the Axl receptor tyrosine kinase in human thyroid carcinoma. *Thyroid: official journal of the American Thyroid Association* **9**, 563–567, doi:[10.1089/thy.1999.9.563](https://doi.org/10.1089/thy.1999.9.563) (1999).
- Linger, R. M., Keating, A. K., Earp, H. S. & Graham, D. K. TAM receptor tyrosine kinases: biologic functions, signaling, and potential therapeutic targeting in human cancer. *Advances in cancer research* **100**, 35–83, doi:[10.1016/S0065-230X\(08\)00002-X](https://doi.org/10.1016/S0065-230X(08)00002-X) (2008).
- Smallridge, R. C. *et al.* American Thyroid Association guidelines for management of patients with anaplastic thyroid cancer. *Thyroid: official journal of the American Thyroid Association* **22**, 1104–1139, doi:[10.1089/thy.2012.0302](https://doi.org/10.1089/thy.2012.0302) (2012).
- Garg, M. *et al.* Sperm-associated antigen 9: a novel diagnostic marker for thyroid cancer. *J Clin Endocrinol Metab* **94**, 4613–4618, doi:[10.1210/jc.2009-0703](https://doi.org/10.1210/jc.2009-0703) (2009).
- Kau, T. R., Way, J. C. & Silver, P. A. Nuclear transport and cancer: from mechanism to intervention. *Nature reviews. Cancer* **4**, 106–117, doi:[10.1038/nrc1274](https://doi.org/10.1038/nrc1274) (2004).
- Lapalombella, R. *et al.* Selective inhibitors of nuclear export show that CRM1/XPO1 is a target in chronic lymphocytic leukemia. *Blood* **120**, 4621–4634, doi:[10.1182/blood-2012-05-429506](https://doi.org/10.1182/blood-2012-05-429506) (2012).
- Alexander, T. B. *et al.* Phase I Study of Selinexor, a Selective Inhibitor of Nuclear Export, in Combination With Fludarabine and Cytarabine, in Pediatric Relapsed or Refractory Acute Leukemia. *Journal of clinical oncology: official journal of the American Society of Clinical Oncology* **34**, 4094–4101, doi:[10.1200/JCO.2016.67.5066](https://doi.org/10.1200/JCO.2016.67.5066) (2016).
- Cheng, Y. *et al.* XPO1 (CRM1) inhibition represses STAT3 activation to drive a survivin-dependent oncogenic switch in triple-negative breast cancer. *Molecular cancer therapeutics* **13**, 675–686, doi:[10.1158/1535-7163.MCT-13-0416](https://doi.org/10.1158/1535-7163.MCT-13-0416) (2014).



41. Kazim, S. *et al.* Selective Nuclear Export Inhibitor KPT-330 Enhances the Antitumor Activity of Gemcitabine in Human Pancreatic Cancer. *Molecular cancer therapeutics* **14**, 1570–1581, doi:[10.1158/1535-7163.MCT-15-0104](https://doi.org/10.1158/1535-7163.MCT-15-0104) (2015).
42. Wasenius, V. M. *et al.* MET receptor tyrosine kinase sequence alterations in differentiated thyroid carcinoma. *The American journal of surgical pathology* **29**, 544–549 (2005).
43. Terrier, P. *et al.* Structure and expression of c-myc and c-fos proto-oncogenes in thyroid carcinomas. *British journal of cancer* **57**, 43–47 (1988).
44. Schmidt, J. *et al.* Genome-wide studies in multiple myeloma identify XPO1/CRM1 as a critical target validated using the selective nuclear export inhibitor KPT-276. *Leukemia* **27**, 2357–2365, doi:[10.1038/leu.2013.172](https://doi.org/10.1038/leu.2013.172) (2013).
45. Mendonca, J. *et al.* Selective inhibitors of nuclear export (SINE) as novel therapeutics for prostate cancer. *Oncotarget* **5**, 6102–6112, doi:[10.18632/oncotarget.2174](https://doi.org/10.18632/oncotarget.2174) (2014).
46. Garg, M. *et al.* Establishment and characterization of novel human primary and metastatic anaplastic thyroid cancer cell lines and their genomic evolution over a year as a primagraft. *The Journal of clinical endocrinology and metabolism* **100**, 725–735, doi:[10.1210/jc.2014-2359](https://doi.org/10.1210/jc.2014-2359) (2015).
47. Garg, M. *et al.* Laminin-5gamma-2 (LAMC2) is highly expressed in anaplastic thyroid carcinoma and is associated with tumor progression, migration, and invasion by modulating signaling of EGFR. *The Journal of clinical endocrinology and metabolism* **99**, E62–72, doi:[10.1210/jc.2013-2994](https://doi.org/10.1210/jc.2013-2994) (2014).
48. Garg, M. *et al.* Sperm-associated antigen 9 is associated with tumor growth, migration, and invasion in renal cell carcinoma. *Cancer research* **68**, 8240–8248, doi:[10.1158/0008-5472.CAN-08-1708](https://doi.org/10.1158/0008-5472.CAN-08-1708) (2008).
49. Garg, M. *et al.* Profiling of somatic mutations in acute myeloid leukemia with FLT3-ITD at diagnosis and relapse. *Blood* **126**, 2491–2501, doi:[10.1182/blood-2015-05-646240](https://doi.org/10.1182/blood-2015-05-646240) (2015).
50. Hayano, T. *et al.* SOX7 is down-regulated in lung cancer. *Journal of experimental & clinical cancer research: CR* **32**, 17, doi:[10.1186/1756-9966-32-17](https://doi.org/10.1186/1756-9966-32-17) (2013).

## Acknowledgements

This work was supported by the Singapore Ministry of Health's National Medical Research Council under its Singapore Translational Research (STaR) Investigator Award to H. Phillip Koeffler (National Research Foundation Singapore and the Singapore Ministry of Education under the Research Centres of Excellence initiative) and Ramalingaswami Fellowship Award to Manoj Garg, Department of Biotechnology, Government of India, Science & Engineering Research Board (SERB; ECR/2016/001519), DST, Government of India.

## Author Contributions

Conceived and designed the experiments: M.G. Performed the experiments: M.G., D.K., A.M., B.S., S.S., S.S., N.R.P., N.B.D., L.W.D. Analyzed the data: M.G., A.M., J.W.S., T.S.G. Contributed reagents/materials/analysis tools: M.G., T.S.G., E.B., S.S., M.K., H.P.K. Contributed to the writing of the manuscript: M.G., H.P.K. All authors reviewed the manuscript.

## Additional Information

**Supplementary information** accompanies this paper at doi:[10.1038/s41598-017-10325-x](https://doi.org/10.1038/s41598-017-10325-x)

**Competing Interests:** E.B., S.S., and M.K. are employees and stockholders of Karyopharm Therapeutics. The remaining authors have no competitive financial interest.

**Publisher's note:** Springer Nature remains neutral with regard to jurisdictional claims in published maps and institutional affiliations.



**Open Access** This article is licensed under a Creative Commons Attribution 4.0 International License, which permits use, sharing, adaptation, distribution and reproduction in any medium or format, as long as you give appropriate credit to the original author(s) and the source, provide a link to the Creative Commons license, and indicate if changes were made. The images or other third party material in this article are included in the article's Creative Commons license, unless indicated otherwise in a credit line to the material. If material is not included in the article's Creative Commons license and your intended use is not permitted by statutory regulation or exceeds the permitted use, you will need to obtain permission directly from the copyright holder. To view a copy of this license, visit <http://creativecommons.org/licenses/by/4.0/>.

© The Author(s) 2017